Human Molecular Genetics, 2013, Vol. 22, No. 24 ***4901–4913***
doi:10.1093/hmg/ddt340
Advance Access published on July 17, 2013

The SNM1B/APOLLO DNA nuclease functions in resolution of replication stress and maintenance of common fragile site stability

Jennifer M. Mason[1,2,†], Ishita Das[3,†], Martin Arlt[1], Neil Patel[2], Stephanie Kraftson[2], Thomas W. Glover[1] and JoAnn M. Sekiguchi[1,2,3,*]

[1]Department of Human Genetics and [2]Department of Internal Medicine and [3]Cellular and Molecular Biology Program, University of Michigan Medical School, Ann Arbor, MI 48109-2200, USA

Received June 3, 2013; Revised July 5, 2013; Accepted July 12, 2013

SNM1B/Apollo is a DNA nuclease that has important functions in telomere maintenance and repair of DNA interstrand crosslinks (ICLs) within the Fanconi anemia (FA) pathway. SNM1B is required for efficient localization of key repair proteins, such as the FA protein, FANCD2, to sites of ICL damage and functions epistatically to FANCD2 in cellular survival to ICLs and homology-directed repair. The FA pathway is also activated in response to replication fork stalling. Here, we sought to determine the importance of SNM1B in cellular responses to stalled forks in the absence of a blocking lesion, such as ICLs. We found that depletion of SNM1B results in hypersensitivity to aphidicolin, a DNA polymerase inhibitor that causes replication stress. We observed that the SNM1B nuclease is required for efficient localization of the DNA repair proteins, FANCD2 and BRCA1, to subnuclear foci upon aphidicolin treatment, thereby indicating SNM1B facilitates direct repair of stalled forks. Consistent with a role for SNM1B subsequent to recognition of the lesion, we found that SNM1B is dispensable for upstream events, including activation of ATR-dependent signaling and localization of RPA, γH2AX and the MRE11/RAD50/NBS1 complex to aphidicolin-induced foci. We determined that a major consequence of SNM1B depletion is a marked increase in spontaneous and aphidicolin-induced chromosomal gaps and breaks, including breakage at common fragile sites. Thus, this study provides evidence that SNM1B functions in resolving replication stress and preventing accumulation of genomic damage.

INTRODUCTION

Replication of the genome is essential for faithful transmission of genetic information to daughter cells and for maintenance of genomic integrity. The DNA replication machinery is highly processive and accurate; however, progression of the replication fork can be impeded by secondary DNA structures or physical blocks, such as DNA interstrand crosslinks (ICLs). Blocked or stalled forks can be stabilized and restarted upon arrest; however, they may also collapse, leading to genomic damage in the form of DNA double-strand breaks (DSBs). Replication-associated DSBs have potential to engage in mutagenic events such as chromosomal deletions or aberrant rearrangements (1,2). Replication stress represents a constant threat to the genome; thus, it is of importance to elucidate the cellular mechanisms that ensure efficient resolution of blocked or stalled replication forks.

SNM1B/Apollo is a DNA nuclease comprising a highly conserved, catalytic metallo-β-lactamase/β-CASP N-terminal domain and a unique C-terminus (3). Previous studies have demonstrated critical functions for its intrinsic 5′-to-3′ exonuclease activity in the processing of leading strand telomeres to protect them from end-to-end joining (4–6). SNM1B also plays important roles in the repair of DNA damage. In this regard, depletion of SNM1B in mammalian cells results in hypersensitivity to ICL-inducing agents such as mitomycin C and a moderate sensitivity to ionizing radiation (7–10). We demonstrated that SNM1B is required for efficient localization of key repair proteins,

*To whom correspondence should be addressed at: 109 Zina Pitcher Place, Box 2200, 2063 BSRB, Ann Arbor, MI 48109-2200, USA. Tel: +1 7347649514; Fax: +1 7347632162; Email: sekiguch@med.umich.edu
†These authors contributed equally to this work.

including the Fanconi anemia (FA) protein, FANCD2, and the homologous recombination proteins, BRCA1 and RAD51, to sites of ICL-induced damage (9).

FA is an inherited genome instability disorder characterized by bone marrow failure, skeletal defects, cancer predisposition and cellular hypersensitivity to ICLs (11,12). There are currently 15 known FA complementation groups (FANCA, B, C, D1/BRCA2, D2, E, F, G, I, J, L, M, N, O, P). A 'core' complex comprising eight FA proteins (FANCA, B, C, E, F, G, L and M) possesses ubiquitin ligase activity and is activated by the presence of ICLs. The core complex monoubiquitinates FANCD2 and FANCI, which localize to chromatin and form subnuclear foci at the sites of damage (11,12). The FA pathway plays central roles in ICL repair, and FA patient cell lines are hypersensitive to ICLs and exhibit spontaneous and replication stress-induced chromosomal aberrations. SNM1B depletion also results in increased levels of spontaneous and ICL-induced chromosomal anomalies, including gaps, breaks and radial structures. The cellular phenotypes of SNM1B-depleted cells parallel those observed in FA cells, and indeed, the functions of SNM1B in ICL repair and maintaining chromosomal stability are epistatic to FANCD2 and FANCI (9).

The FA pathway is also activated in response to replication fork slowing or stalling (13). The mechanisms involved in resolving replication stress are distinct from those required for removal or bypass of ICLs and are not fully defined. One outstanding question is the identification of DNA nucleases involved in processing the nascent DNA strands to facilitate replication restart or repair upon fork collapse (14). SNM1B is one of several candidate nucleases that may participate in nucleolytic processing of replication intermediates. It has been demonstrated to form complexes with proteins that localize to and function in the repair of stalled forks. SNM1B interacts directly with MRE11 (7), an endo/exonuclease that facilitates replication fork restart (15,16) and localizes to stalled replication forks (17–19). MRE11 also catalyzes enhanced resection of unprotected stalled replication forks (20–22). In addition, SNM1B interacts with the FA proteins, FANCD2 (7) and FANCP/SLX4 (23). Monoubiquitinated FANCD2 localizes to sites of stalled forks (13) and functions in stabilizing and protecting stalled forks from extensive nucleolytic degradation (22). FANCP/SLX4 is a scaffold protein that interacts with several structure-specific nucleases and regulates their activities in response to different types of DNA damage, including replication stress (24–28). Like FANCD2, FANCP/SLX4 functions epistatically to SNM1B in repair of ICLs (23).

Given the evidence that SNM1B functions within the FA pathway in the repair of ICLs and interacts with proteins involved in resolving replication stress, we have examined the importance of the SNM1B nuclease in the repair of stalled forks. We find that depletion of SNM1B from human cell lines results in hypersensitivity to the DNA polymerase inhibitor, aphidicolin, which causes replication fork slowing and stalling. We demonstrate that SNM1B-depleted cells are not defective for sensing or signaling aphidicolin-induced DNA damage. However, the SNM1B nuclease is required for efficient localization of key repair proteins, FANCD2 and BRCA1, to stalled replication forks. We also observe that SNM1B-depleted cells exhibit elevated levels of spontaneous and aphidicolin-induced gaps and breaks, including increased instability at the common fragile sites, FRA3B and FRA16D. These findings provide evidence that the SNM1B nuclease plays critical roles in the resolution of stalled replication forks to maintain genome stability.

RESULTS

Impact of SNM1B depletion on cellular survival and signaling in response to aphidicolin treatment

We examined the impact of SNM1B depletion on cellular survival upon exposure to the DNA polymerase inhibitor, aphidicolin. Wild-type human fibroblasts were transfected with a previously characterized siRNA specific for SNM1B (siSnm1B-1) or a non-silencing (NS) siRNA control (9). At 48 h post-transfection, cultures were treated with 0, 0.25, 0.5 and 1 μM aphidicolin for 24 h, and the number of surviving cells was quantitated. We observed that SNM1B-depleted fibroblasts exhibited significantly reduced survival after aphidicolin treatment when compared with controls (Fig. 1A). To confirm these results, we examined aphidicolin sensitivity in HeLa cells transfected with siSnm1B-1 and a distinct siRNA, siSnm1B-2, that binds to a downstream sequence within the mRNA (9). We observed that depletion of SNM1B with either siRNA significantly reduced survival of HeLa cells upon exposure to aphidicolin (Supplementary Material, Fig. S1A). We further examined aphidicolin sensitivity in HCT116 cells transfected with siSnm1B-1 and observed reduced survival of HCT116 cells depleted of SNM1B in response to aphidicolin treatment (Supplementary Material, Fig. S1B).

The presence of long stretches of ssDNA generated upon replication fork stalling activates signaling pathways, and defects in DNA damage sensing or signaling can manifest as decreased cellular survival. Thus, we examined the cellular responses to the inhibition of DNA polymerase activity in SNM1B-depleted cells. The ATR protein kinase plays a central role in initiating the cellular responses to replication stress. The canonical signaling pathway is initiated upon binding of the RPA heterotrimeric complex to ssDNA at stalled forks and recruitment of ATR to ssDNA-RPA via its binding partner, ATRIP. Subsequent activation of ATR-ATRIP results in the phosphorylation of downstream substrates to potentiate damage-induced signaling (29).

One key signaling event indicative of ATR activation in response to replication stress is phosphorylation of the effector protein kinase, CHK1 (30). To assess the importance of SNM1B in ATR-dependent signaling, we depleted SNM1B in the HCT116 human colon cancer cell line and assessed pCHK1 S317 levels upon exposure to aphidicolin (0.3 μM) by western blotting. We observed that aphidicolin treatment induced phosphorylation of CHK1 in both siSnm1B-1- and NS-transfected cells, and the levels of CHK1 p-S317 were approximately equivalent (Fig. 1B). ATR-dependent phosphorylation of the RPA32 subunit is another well-characterized event in response to replication stress. Thus, we next examined levels of RPA32 phosphorylation and observed that aphidicolin induced similar levels of p-RPA in the SNM1B-depleted cells compared with controls (Fig. 1B).

PCNA is the homotrimeric sliding clamp that tethers DNA polymerases to replication forks. It becomes monoubiquitinated in a CHK1-dependent, ATR-independent manner and facilitates translesion DNA synthesis upon replication fork stalling (31,32). We found that SNM1B depletion did not have a significant impact on Ub-PCNA levels compared with NS-transfected

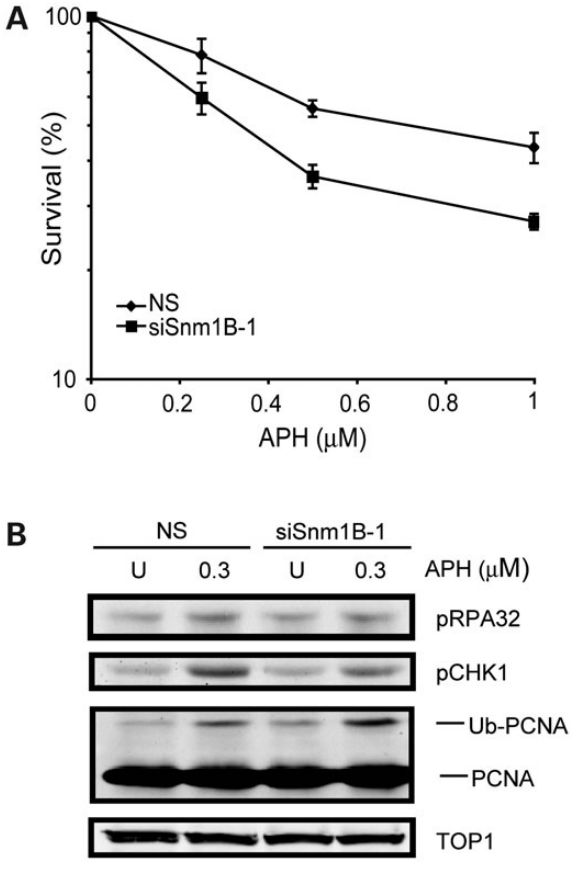

Figure 1. Cellular responses to replication stress upon SNM1B depletion. (**A**) Cellular survival in response to aphidicolin treatment. Wild-type human fibroblasts transfected with NS or siSnm1B-1 were treated with the indicated doses of aphidicolin for 24 h at 48 h post-transfection. Cells were allowed to proliferate for 5–7 days. Percent survival was determined compared with an untreated control. The graph represents the average of three independent experiments. Error bars: standard deviation. (**B**) ATR-dependent signaling in SNM1B-depleted cells. NS- or siSnm1B-1-transfected HCT116 cells were treated with aphidicolin (0.3 μM) for 24 h, and whole-cell lysates were analyzed by western blotting. Phosphorylation of RPA (pRPA32) and CHK1 (pCHK1) and monoubiquitination of PCNA (Ub-PCNA) were examined. Representative blots from at least six independent experiments are shown. Topoisomerase I (TOP1), loading control; U, untreated controls.

controls (Fig. 1B). These results indicate that SNM1B does not play a critical role in the cellular signaling response to replication stress, including PCNA ubiquitination and ATR-dependent phosphorylation of CHK1 and RPA32. Consistent with these findings, we observed that SNM1B-depleted and control cells exhibit similar proportions of cells accumulating in S phase in response to low-dose aphidicolin treatment (Supplementary Material, Fig. S2). However, higher percentages of sub-G1 cells were observed in SNM1B-depleted cells, consistent with the reduced cell survival observed in Figure 1A (Supplementary Material, Fig. S2).

SNM1B is not required for localization of RPA, γH2AX and the MRN complex to aphidicolin-induced subnuclear foci

RPA localization to regions of ssDNA at replication forks can be visualized as punctate, subnuclear foci by immunofluorescence microscopy (Fig. 2A). We examined the impact of SNM1B depletion on RPA foci formation in HCT116 cells exposed to 0.3 μM aphidicolin at early (6 h) and later (24 h) time points. Upon aphidicolin treatment, we observed an ∼2-fold increase in RPA foci-positive cells in both siSnm1B-1- and NS-transfected cells at 6 h and an even further increase at 24 h (Fig. 2A). We noted that the percentages of aphidicolin-induced RPA foci-positive cells in SNM1B-depleted cells were consistently higher at 24 h compared with controls. These findings demonstrate that SNM1B is not required for RPA localization and suggest that SNM1B depletion results in increased ssDNA formation upon replication fork stalling.

The histone variant, H2AX, is phosphorylated by ATR in response to stalled or blocked replication forks. Recent studies have demonstrated that phosphorylated H2AX (γH2AX) is localized at stalled forks prior to the detection of DNA breaks and is required for efficient recruitment of other repair proteins, including FANCD2 and BRCA1 (33–35). We observed that aphidicolin treatment of siSnm1B-1- and NS-transfected cells induced γH2AX foci formation (Fig. 2B). However, SNM1B depletion did not impact the percentage of γH2AX foci-positive cells at either 6 or 24 h post-aphidicolin treatment compared with controls.

MRE11 is a DNA nuclease that functions within the context of the heterotrimeric MRN protein complex. MRN plays central roles in the repair of DNA DSBs, and it also has functions during DNA replication. MRE11 and NBS1 have been demonstrated to co-localize with RPA, γH2AX and FANCD2 at stalled replication forks (17–19), and both MRE11 and NBS1 physically interact with RPA (36). Previous studies identified physical interactions between SNM1B and the MRE11 and RAD50 components of MRN (7). Therefore, we next examined the impact of SNM1B depletion on replication stress-induced MRE11 and NBS1 foci formation. We found that, similar to RPA and γH2AX foci, MRE11 and NBS1 localization to sites of stalled forks was not dependent on SNM1B (Fig. 2C).

Impact of SNM1B depletion on FANCD2 monoubiquitination, chromatin localization and foci formation

The FA protein, FANCD2, plays a central role in cellular responses to stalled forks. It forms a stable complex with FANCI, and both proteins undergo monoubiquitination by the FA core complex in response to genotoxic stress. Monoubiquitinated FANCD2-FANCI becomes associated with nuclear chromatin and subsequently assembles into foci. FANCD2 then recruits additional repair factors required for the resolution of stalled replication forks (37,38). We examined the levels of aphidicolin-induced FANCD2 ubiquitination (FANCD2-Ub) and chromatin localization of FANCD2-Ub in SNM1B-depleted cells. The cytosolic and chromatin-bound proteins were fractionated from siSnm1B-1- and NS-transfected cells, and the levels of FANCD2 (S) and FANCD2-Ub (L) in each fraction were determined by western blotting. We observed that SNM1B depletion did not significantly impact the extent of monoubiquitination of FANCD2 (FANCD2-L) upon aphidicolin treatment, nor did it affect the accumulation of FANCD2-Ub in the chromatin fraction (P1) (Fig. 3A).

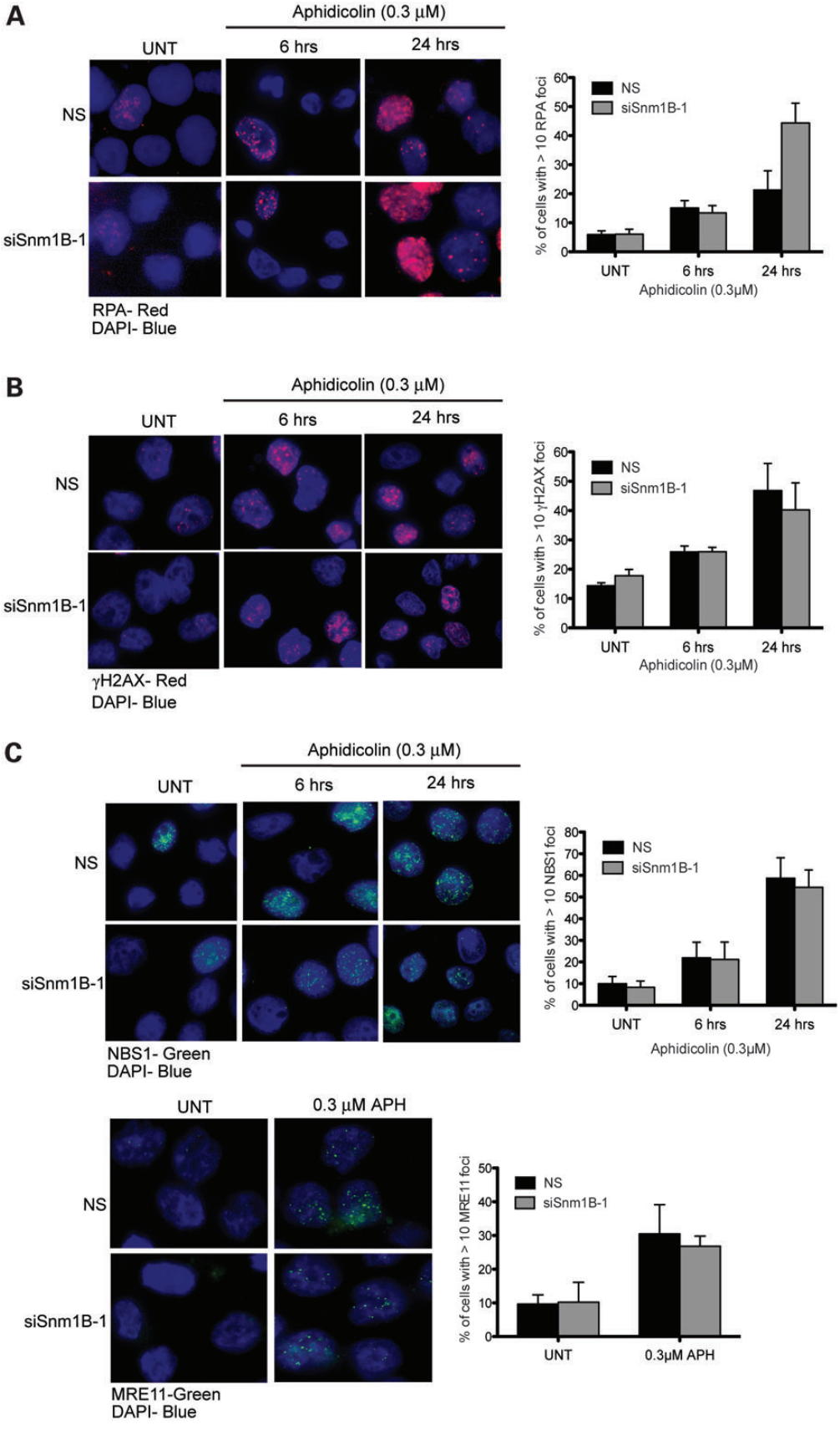
A
Aphidicolin (0.3 μM)
UNT
6 hrs
24 hrs
NS
siSnm1B-1
RPA- Red
DAPI- Blue
% of cells with > 10 RPA foci
NS
siSnm1B-1
UNT
6 hrs
24 hrs
Aphidicolin (0.3μM)
B
Aphidicolin (0.3 μM)
UNT
6 hrs
24 hrs
NS
siSnm1B-1
γH2AX- Red
DAPI- Blue
% of cells with > 10 γH2AX foci
NS
siSnm1B-1
UNT
6 hrs
24 hrs
Aphidicolin (0.3μM)
C
Aphidicolin (0.3 μM)
UNT
6 hrs
24 hrs
NS
siSnm1B-1
NBS1- Green
DAPI- Blue
% of cells with > 10 NBS1 foci
NS
siSnm1B-1
UNT
6 hrs
24 hrs
Aphidicolin (0.3μM)
UNT
0.3 μM APH
NS
siSnm1B-1
MRE11-Green
DAPI- Blue
% of cells with > 10 MRE11 foci
NS
siSnm1B-1
UNT
0.3μM APH

We next examined replication stress-induced FANCD2 foci in siSnm1B-1- and NS-transfected cells exposed to 0.3 μM aphidicolin. We observed that the percentage of control cells containing FANCD2 foci increased ~3.5- and 13-fold at 6 and 24 h of aphidicolin treatment, respectively (Fig. 3B). In contrast, SNM1B depletion markedly reduced the percentage of aphidicolin-induced FANCD2 foci to ~50% of controls at both 6 and 24 h ($P < 0.01$). We observed a similar decrease in FANCD2 formation in HCT116 cells transfected with siSnm1B-2 upon aphidicolin treatment (Supplementary Material, Fig. S3A). Furthermore, we examined replication stress-induced FANCD2 foci in HeLa cells and confirmed that depletion of SNM1B significantly impairs recruitment to sites of stalled forks. We observed a decrease in the percentage of HeLa cells with FANCD2 foci to ~50 and 35% of controls upon transfection with siSnm1B-1 and siSnm1B-2, respectively (Supplementary Material, Fig. S3B). Thus, these results clearly establish that SNM1B is required for efficient assembly of FANCD2 into DNA repair foci; however, it is dispensable for activation and chromatin localization of FANCD2.

SNM1B possesses intrinsic 5′-to-3′ DNA exonuclease activity on single- and double-strand substrates (4,5,39,40). This nuclease activity is required for DNA end-resection of telomeres to generate 3′ single-strand overhangs for protection against inappropriate end-to-end joining of chromosomes (4,5,39). We assessed the importance of SNM1B nuclease activity on localization of FANCD2 to DNA repair foci in response to replication stress. To this end, we generated an siRNA-resistant lentiviral SNM1B cDNA with a C-terminal V5 epitope tag and mutated a residue within the highly conserved metallo-β-lactamase domain required for nucleolytic activity, D14N (Fig. 4A, Supplementary Material, Fig. S4A and B). This residue has been previously demonstrated to be essential for SNM1B 5′-to-3′ exonuclease activity *in vitro* (4,41) and for the functions of SNM1B in telomere processing *in vivo* (4,41). The SNM1B-D14N mutant and wild-type siRNA-resistant cDNAs were expressed from a construct harboring an IRES-GFP cassette, and cells expressing GFP were sorted and cultured. We confirmed the expression of the siRNA-resistant cDNAs by immunoblotting using anti-V5 antibodies and observed both the wild-type and SNM1B-D14N proteins in NS- and siSnm1B-1-transfected cells (Supplementary Material, Fig. S4C).

We observed that the wild-type SNM1B-expressing cells fully complemented the defect in aphidicolin-induced FANCD2 foci formation in siSnm1B-transfected cells (Fig. 4B). In contrast, the nuclease-deficient SNM1B-D14N construct did not complement this defect and exhibited a significantly lower percentage of FANCD2 foci-containing cells (45 versus 22%, $P < 0.05$; wild-type versus SNM1B-D14N, respectively). These findings indicate that the nucleolytic activity intrinsic to SNM1B facilitates the localization of FANCD2-Ub to stalled replication forks.

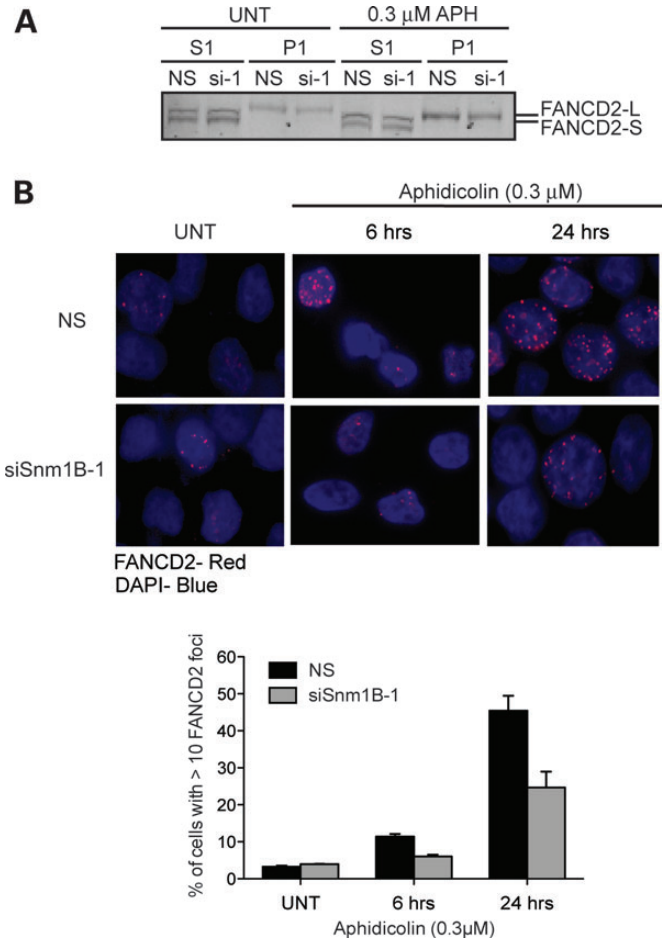

Figure 3. Replication stress-induced FANCD2 foci formation is impaired in SNM1B-depleted cells. (**A**) FANCD2 monoubiquitination in SNM1B-depleted cells. HCT116 cells transfected with NS or siSnm1B-1 (si-1) were treated with aphidicolin (0.3 μM) for 24 h. Cells were harvested, and the soluble (S1) and chromatin-associated (P1) proteins were fractionated. Western blotting to detect the unmodified (FANCD2-S) and monoubiquitinated (FANCD2-L) forms of FANCD2 was performed using α-FANCD2 antibodies. UNT, untreated controls. (**B**) FANCD2 foci formation. HCT116 cells transfected with NS or siSnm1B-1 were treated with aphidicolin (0.3 μM) for 6 or 24 h, as indicated. The average percentage of cells containing more than 10 FANCD2 foci (red) is plotted. The results represent data from three independent experiments; at least 100 cells were scored from each experiment. Nuclei, DAPI-stained (Blue). Error bars, SEM. UNT, untreated controls.

Impact of SNM1B depletion on BRCA1 localization to DNA repair foci

FANCD2 co-localizes with the breast cancer-suppressor protein, BRCA1, in response to UV-induced stalled replication

Figure 2. SNM1B is not required for the localization of RPA, γH2AX and the MRN complex to aphidicolin-induced subnuclear foci. (**A**) RPA foci formation in SNM1B-depleted cells. RPA foci (red fluorescence) were quantitated in SNM1B-depleted and control HCT116 cells exposed to aphidicolin (0.3 μM) for 6 or 24 h. The average percentage of cells containing more than 10 RPA foci is plotted. The results represent data from at least three independent experiments; at least 100 cells were scored from each experiment. Nuclei, DAPI-stained (blue). Error bars, SEM; UNT, untreated controls. (**B**) γH2AX foci formation in SNM1B-depleted cells. γH2AX foci (red) were quantitated in SNM1B-depleted and control HCT116 cells treated with aphidicolin for 6 or 24 h, as described in (A). (**C**) NBS1 and MRE11 foci formation in SNM1B-depleted cells. NBS1 foci (green) were quantitated in SNM1B-depleted and control HeLa cells treated with aphidicolin for 6 or 24 h, as described in (A). MRE11 foci (green) were quantitated in SNM1B-depleted and control HCT116 cells treated with aphidicolin for 24 h, as described in (A).

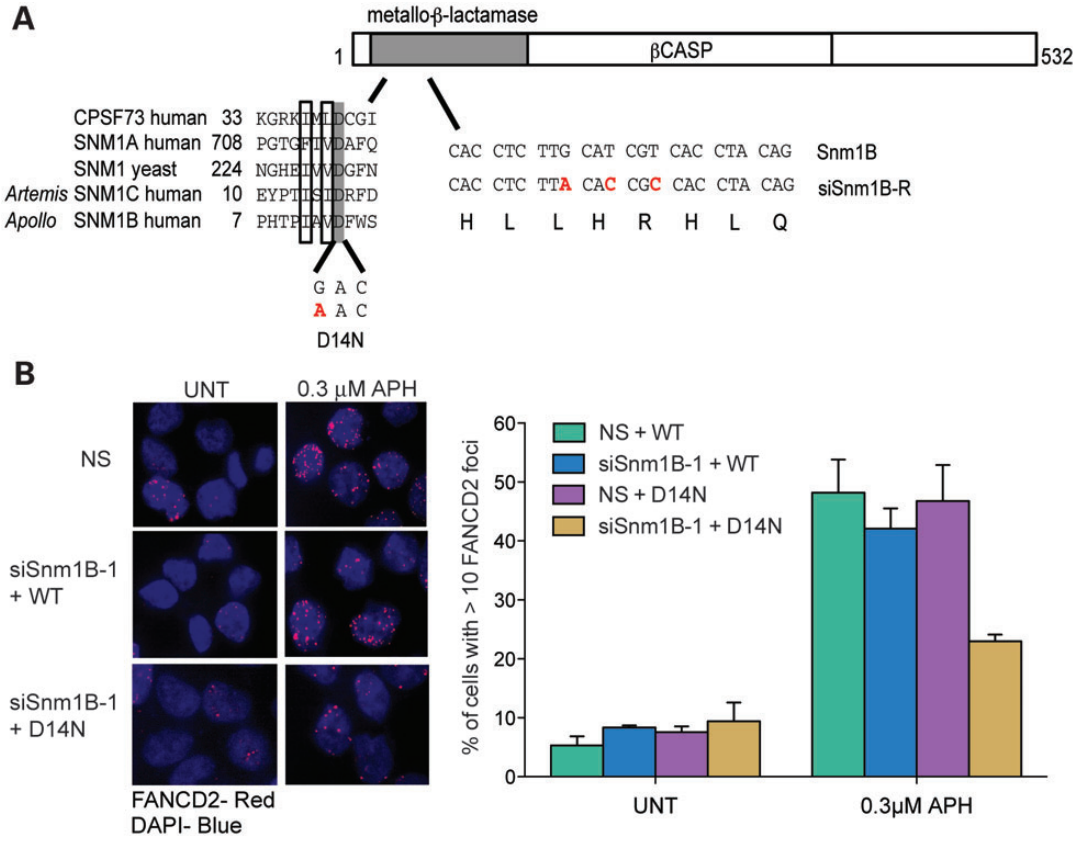

Figure 4. SNM1B nuclease activity is required for efficient FANCD2 foci formation. (**A**) Nuclease-deficient SNM1B cDNA. The diagram of SNM1B cDNA encoding the conserved metallo-β-lacatamase/βCASP domain. Alignment between the *Saccharomyces cerevisiae* and *Homo sapiens* orthologous amino acid sequences of βCASP family members adjacent to the inactivating D14N mutation is shown. Identical residues, gray box; conserved residues, open boxes. Base changes within the target region of the SNM1B siRNA are indicated below the wild-type cDNA sequence as siSnm1B-R (resistant). (**B**) FANCD2 foci formation with nuclease-deficient SNM1B. HCT116 cells transduced with WT-SNM1B-IRES-GFP (WT) or D14N-SNM1B-IRES-GFP (D14N) retroviruses were sorted, then transfected with NS or siSnm1B-1 and treated with aphidicolin (0.3 μM) for 24 h. FANCD2 foci (red) were visualized by immunofluorescence (left panels). The percentage of cells with more than 10 FANCD2 foci were quantitated (right panel). The graph represents the results from at least three independent experiments; at least 100 cells were scored from each experiment. Nuclei, DAPI-stained (Blue). Error bars, SEM. UNT, untreated controls.

forks, and its localization is dependent on BRCA1 (35). Recently, BRCA1 has also been demonstrated to play central roles in stabilizing replication forks prior to collapse (22). Given our observations that SNM1B is required for FANCD2 foci formation in response to replication stress, we examined the impact of SNM1B depletion on BRCA1 localization. Upon exposure to aphidicolin, we observed a significant, ∼5-fold, increase in the percentage of control cells containing BRCA1 foci ($P < 0.008$) (Fig. 5A). However, BRCA1 foci formation was markedly impaired in siSnm1B-1-transfected HCT116 cells. We observed a minimal increase in replication stress-induced localization (∼1.5-fold), and the percentage of aphidicolin-induced BRCA1 foci-containing cells was significantly lower compared with controls ($P < 0.05$). We observed a similar defect in BRCA1 foci formation in HeLa cells transfected with siSnm1B-1, which reduced the percentage of cells with aphidicolin-induced BRCA1 foci to 50% of controls (Supplementary Material, Fig. S5). This impairment in the localization of BRCA1 to sites of stalled forks was fully complemented upon expression of the siRNA-resistant SNM1B cDNA (Fig. 5B). Together, these findings demonstrate that SNM1B is required for efficient recruitment of the key repair proteins, BRCA1 and FANCD2, to sites of stalled replication forks.

SNM1B localizes to subnuclear foci upon aphidicolin treatment

Based on our observations that depletion of SNM1B impairs localization of FANCD2 and BRCA1 to aphidicolin-induced subnuclear foci, we hypothesized that SNM1B may be recruited to sites of stalled forks to facilitate repair. Thus, we treated cells expressing V5-tagged SNM1B with 0.3 μM aphidicolin and examined SNM1B foci formation. We observed a marked 8-fold increase in cells containing SNM1B foci upon exposure to aphidicolin (Fig. 6). These findings indicate that, similar to other proteins required for the resolution of replication stress, SNM1B localizes to stalled forks to facilitate repair.

SNM1B prevents accumulation of spontaneous and replication stress-induced chromosome damage

Defects in the resolution of stalled replication can result in fork collapse and the generation of DNA DSB intermediates that undergo repair via RAD51-mediated homologous recombination. Inefficient repair of collapsed forks results in the accumulation of gaps and breaks, and these DNA lesions accumulate in

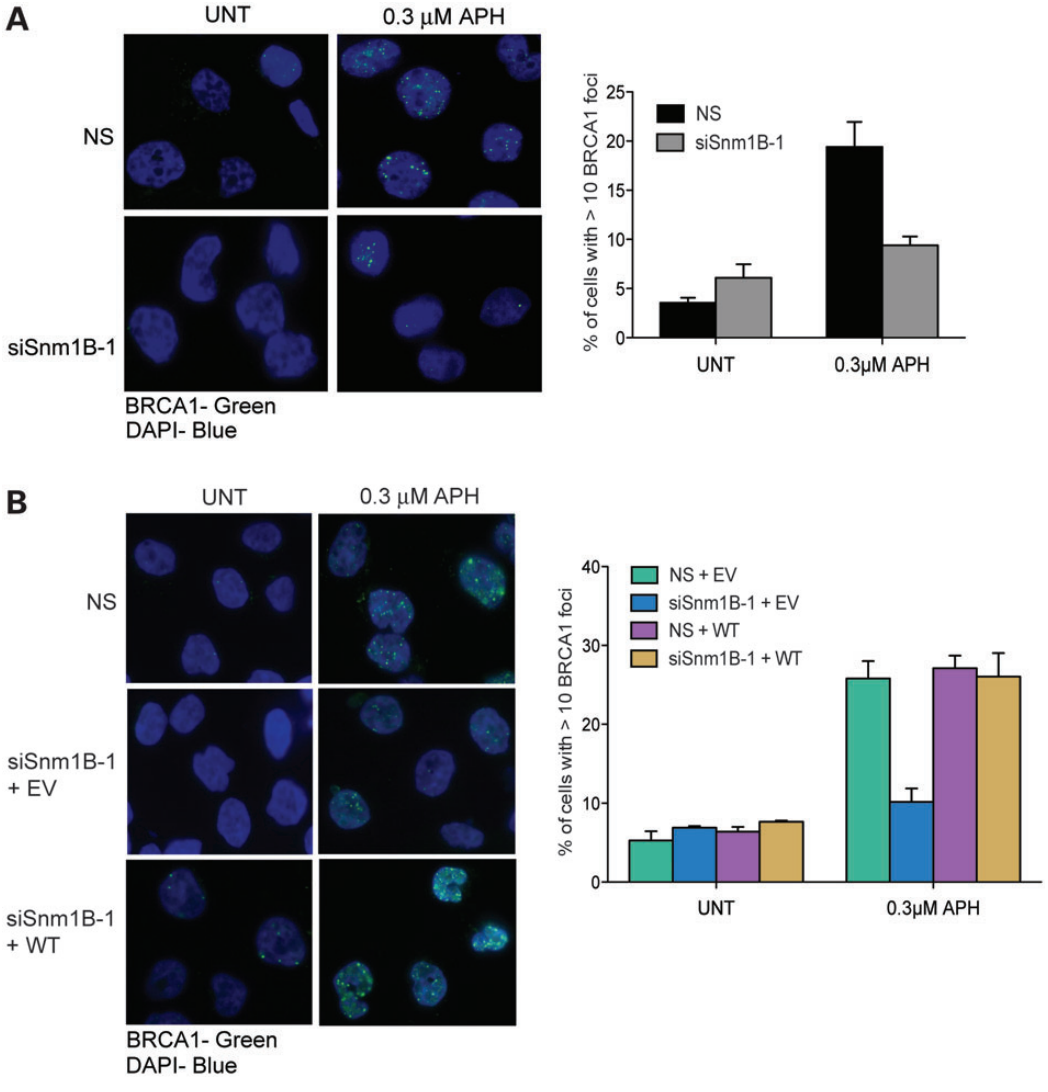

Figure 5. Replication stress-induced BRCA1 foci formation is impaired in SNM1B-deficient cells. (**A**) BRCA1 foci formation. HCT116 cells transfected with NS or siSnm1B-1 were treated with aphidicolin (0.3 μM) for 24 h. The percentage of cells containing more than 10 BRCA1 foci (green) was determined. The graph represents average of four independent experiments; at least 100 cells were scored from each experiment. (**B**) Complementation of defective BRCA1 foci formation. HCT116 cells transduced with pLL-IRES-GFP empty vector (EV) or WT-SNM1B-IRES-GFP (WT) retroviruses were sorted, then transfected with NS or siSnm1B-1 and treated with aphidicolin (0.3 μM) for 24 h. BRCA1 foci (green) were visualized by immunofluorescence (left panels). The percentage of cells with more than 10 BRCA1 foci were quantitated (right panel). The graph represents the results from two independent experiments; at least 100 cells were scored from each experiment. Nuclei, DAPI-stained (Blue). Error bars, SEM. UNT, untreated controls.

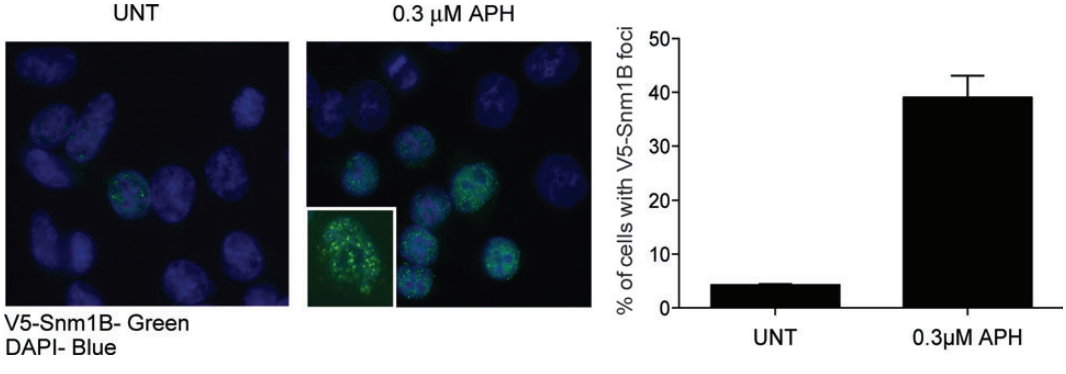

Figure 6. SNM1B forms subnuclear foci in response to aphidicolin. HCT116 cells transduced with WT-SNM1B-IRES-GFP (WT) retroviruses were sorted and treated with aphidicolin (0.3 μM) for 24 h. V5-SNM1B foci (green) were visualized by immunofluorescence (left panels). The average percentage of cells with V5-SNM1B foci was quantitated, and the percentage of cells containing more than five foci is plotted (right panel). The graph represents the results from four independent experiments; at least 100 cells were scored from each experiment. Nuclei, DAPI-stained (Blue). Error bars, SEM. UNT, untreated controls.

cells defective in responses to replication stress, including ATR, CHK1 and FANCD2 deficiencies (13,42–44). Therefore, we examined the impact of SNM1B depletion on spontaneous and aphidicolin-induced gaps and breaks.

We observed that SNM1B depletion in HCT116 cells resulted in significantly elevated levels of spontaneous gaps and breaks compared with controls, as previously reported (7,9,10,45) (Fig. 7A). Untreated NS-transfected cells harbored an average of 0.17 gaps and breaks per metaphase, whereas siSnm1B-1-transfected cells contained ~3-fold more anomalies (0.5 gaps/breaks per metaphase) (Fig. 7B). SNM1B-depleted cells exhibited a dose-dependent increase in gaps/breaks, and at 0.5 μM aphidicolin, siSnm1B-1-transfected cells harbored a substantially higher average number of anomalies per metaphase compared with NS-transfected controls (5 versus 1.7 gaps/breaks per metaphase, respectively; Fig. 7B). A Poisson distribution analysis of the number of spontaneous and aphidicolin-induced gaps/breaks revealed that the differences in mean rate of anomalies in SNM1B-depleted versus control cells were significant in all cases ($P < 0.001$; Fig. 7C).

We note that ~26% of metaphases scored in SNM1B-depleted cells treated with 0.5 μM aphidicolin contained greater than 20 gaps and breaks per metaphase, and in some cases, the number of anomalies was too numerous to quantitate. In contrast, only 5% of control metaphases exhibited greater than 20 gaps/breaks at this aphidicolin dose (Supplementary Material, Fig. S6). These metaphases were not included in the quantitative analyses; therefore, the phenotypes graphically shown underestimate the extent of replication stress-induced chromosomal damage in SNM1B-depleted cells (Fig. 7B and C). Together, these findings demonstrate a critical role for SNM1B in preventing chromosomal gaps/breaks in response to replication perturbation.

SNM1B is required to suppress spontaneous and replication stress-induced common fragile site expression

Common fragile sites are genomic loci that recurrently exhibit gaps and breaks on metaphase chromosomes in response to partial replication inhibition (46). Thus, we hypothesized that

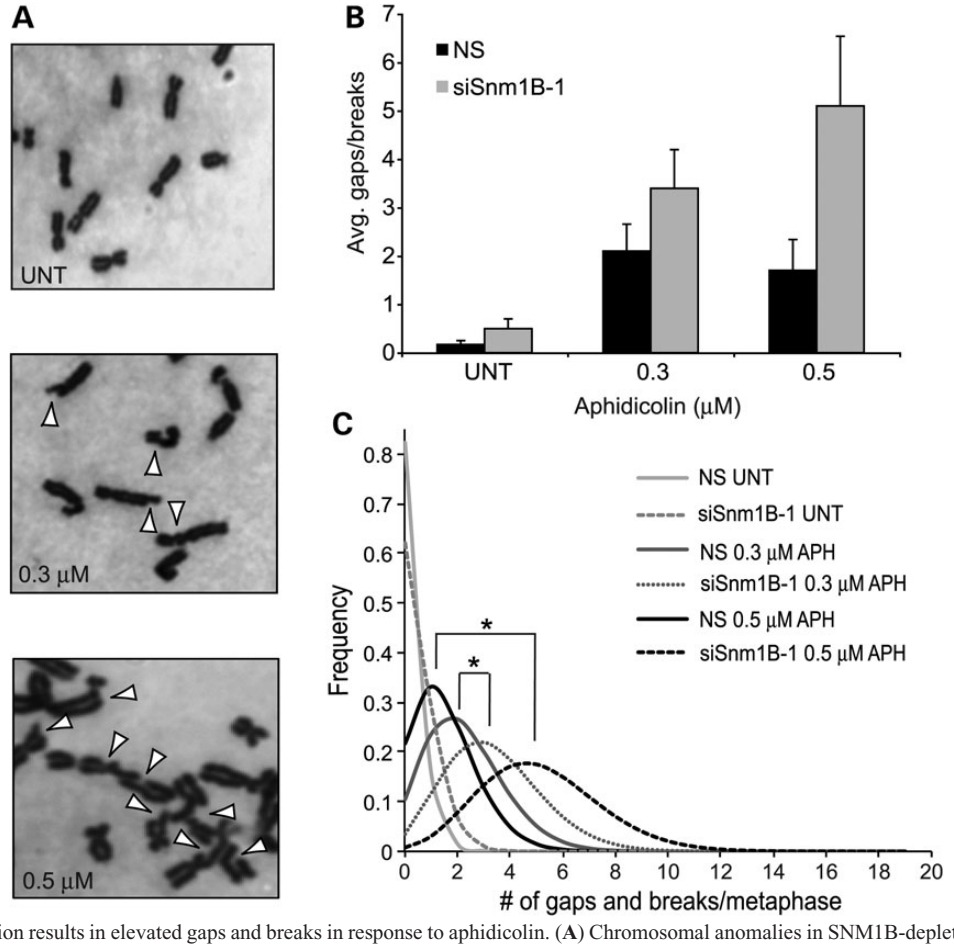

Figure 7. SNM1B depletion results in elevated gaps and breaks in response to aphidicolin. (**A**) Chromosomal anomalies in SNM1B-depleted cells. Representative Giemsa-stained metaphases from SNM1B-depleted HCT116 cells that were untreated (UNT) or were treated with aphidicolin (0.3 or 0.5 μM) for 24 h prior to harvesting. Arrows indicate chromosomes with gaps or breaks. (**B**) Quantitation of gaps and breaks in SNM1B-depleted cells. Graphical representation of the average number of gaps/breaks in metaphase chromosomes that were untreated or treated with aphidicolin. The graph represents data from three independent experiments with SEM. (**C**) Poisson distributions of gaps and breaks. Poisson distributions illustrating the frequencies of gaps and breaks per metaphase observed in untreated (light gray), 0.3 μM (dark gray) and 0.5 μM (black) aphidicolin-treated NS (solid) and siSnm1B-1 (dotted)-transfected cells ($P < 0.001$). Metaphases containing more than 20 gaps/breaks were not included (see Supplementary Material, Fig. S6).

SNM1B depletion would result in increased common fragile site instability. Two of the most frequently expressed common fragile sites in the human genome are FRA3B and FRA16D, located at 3p14.2 and 16q23, respectively (46). We examined the impact of SNM1B depletion on the frequency of spontaneous and aphidicolin-induced instability at both FRA3B and FRA16D (46), using a fluorescence *in situ* hybridization (FISH) approach with YAC/BAC probes located at the fragile sites (13).

We observed low or undetectable levels of chromosomal breaks within either the FRA3B (1.4% of FRA3B signals with breaks) or FRA16D (0% of signals with breaks) loci in metaphases from NS-transfected, untreated cells (Fig. 8A and B). In contrast, SNM1B depletion significantly increased the frequency of spontaneous breaks at both FRA3B and FRA16D (to 6.9 and 4.6%, respectively). Aphidicolin treatment of SNM1B-depleted cells leads to a further increase in fragile site instability, and the percentages of FRA3B (22%) and FRA16D (10%) signals localized to a break were consistently higher in comparison with NS-transfected controls (~7% for both FRA3B and FRA16D) (Fig. 8A and B). These findings indicate that SNM1B is important for maintaining fragile site stability not only in response to partial inhibition of DNA polymerase, but also in the context of unperturbed DNA replication.

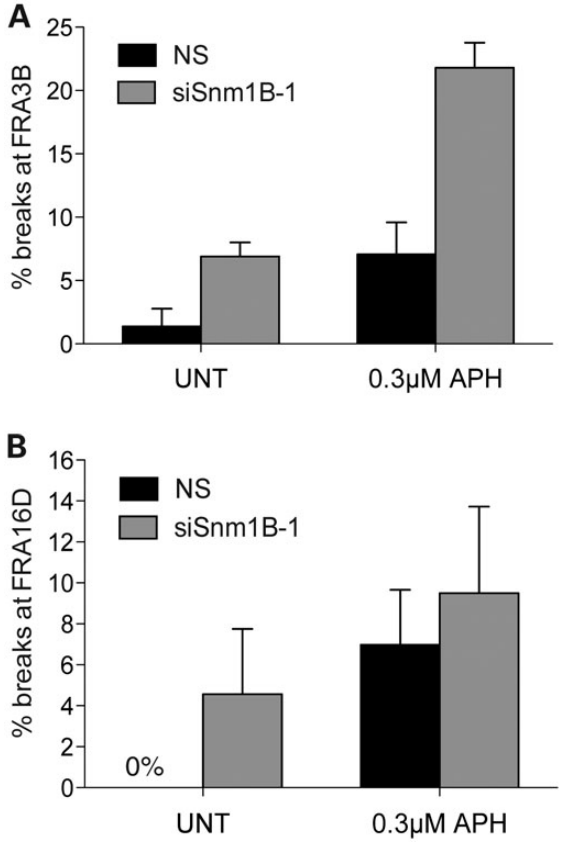

Figure 8. SNM1B-depleted cells exhibit increased fragile site expression. HCT116 cells were transfected with NS or siSnm1B-1 and treated with aphidicolin (0.3 μM) for 24 h. Untreated samples were used as controls. FISH analyses using YAC/BAC probes were used to determine the frequency of FRA3B and FRA16D expression. (**A**) Expression of FRA3B in SNM1B-depleted cells. Quantitation of FRA3B expression in NS- and siSnm1B-1-transfected cells treated with 0 (UNT) or 0.3 μM aphidicolin. The bar graph represents average percentage of FRA3B signals localized at breaks from at least three independent experiments; Error bars, SEM. (**B**) Expression of FRA16D in SNM1B-depleted cells. Quantitation of FRA16D expression in NS- and siSnm1B-1-transfected cells treated with 0 (UNT) or 0.3 μM aphidicolin. The bar graph represents average percentage of FRA16D signals localized at breaks from at least three independent experiments; Error bars, SEM.

DISCUSSION

In this study, we provide evidence that the SNM1B/Apollo DNA nuclease has critical functions in the resolution of DNA replication stress. We demonstrate that SNM1B is required for cellular survival in response to replication fork stalling. Depletion of SNM1B does not significantly affect ATR-dependent signaling events or localization of proteins involved in the early response to stalled replication forks prior to DSB formation, i.e. RPA, γH2AX and the MRN complex (20,33). In contrast, SNM1B depletion markedly impairs localization of the critical repair proteins, FANCD2-Ub and BRCA1, to replication stress-induced foci. We also found that SNM1B protects the genome from the accumulation of spontaneous and aphidicolin-induced gaps and breaks, including those at common fragile sites. Thus, our findings demonstrate that SNM1B is dispensable for the recognition of the lesion and the activation of the DNA damage response, but is required during the downstream events to facilitate fork stabilization and repair.

During DNA synthesis, the replication fork frequently encounters barriers that impede progression and cause stalling. These barriers can be in the form of blocking DNA lesions or intrinsic, natural impediments to fork progression, such as secondary DNA structures, highly transcribed regions or tightly bound proteins (47–49). Evidence indicates that the replication machinery remains stably associated with the stalled fork and is poised for replication restart. Prolonged stalling or defects in maintaining fork stability can lead to fork collapse and increased genome instability, including chromosomal deletions, duplications or more complex rearrangements. Previous studies have provided evidence that FANCD2, BRCA1, BRCA2 and RAD51 act in concert to stabilize stalled replication forks by protecting nascent DNA from excessive MRE11-dependent resection (20–22,50). We demonstrated impaired recruitment of FANCD2 and BRCA1 to sites of aphidicolin-induced stalled forks in SNM1B-depleted cells (Fig. 3B and 5). This defect in FANCD2/BRCA1 localization could result in excessive resection, which would manifest as long stretches of ssDNA and an increased percentage of RPA-positive cells, as observed in our study (Fig. 2A). Thus, our findings suggest that SNM1B facilitates the stabilization and repair of stalled replication forks.

We find that the intrinsic SNM1B nuclease activity plays an important role during the resolution of stalled replication forks, as the D14N mutant protein is unable to restore aphidicolin-induced FANCD2 foci formation. Although the precise functions of SNM1B nuclease activity during replication have yet to be uncovered, the roles of SNM1B in telomere processing provide some insights. At telomeres, the 5′-to-3′ exonuclease activity of SNM1B has been demonstrated to be involved in generating the 3′ overhang at leading strand telomeres (4–6). SNM1B nuclease activity could also relieve topological strain induced during replication of telomeres (41). Both SNM1B-catalyzed end-resection and/or regulation of DNA topology may have

relevance at replication forks. In this regard, unregulated unwinding of DNA ahead of a stalled fork, caused by uncoupling of polymerase and helicase activities, can result in positive supercoiling that promotes fork regression (51). SNM1B may play a role in relieving this torsional strain, similar to its proposed roles in unwinding superhelical strain at telomeres (41). Alternatively, SNM1B-mediated 5′-to-3′ exonucleolytic processing of nascent lagging strand DNA could generate ssDNA regions necessary for the loading of fork-stabilizing proteins, such as FANCD2, BRCA1 and RAD51 (20,22), or degrade reversed forks to facilitate replication restart (2). It is likely that SNM1B collaborates with other DNA nucleases at stalled forks, as it physically interacts with MRE11 (7) and MUS81 (23) and the nuclease scaffold protein, SLX4, each of which has been implicated in the repair of blocked or stalled forks (26,52,53). Detailed molecular analyses of nascent DNA strand degradation and synthesis will provide significant insights into the roles of SNM1B and functional interactions with other DNA nucleases during the resolution of replication stress.

Our studies demonstrated that SNM1B is required for preventing chromosomal damage, including common fragile site instability, not only in response to aphidicolin-induced replication inhibition, but also during unperturbed DNA replication. Common fragile sites are difficult to replicate loci in the genome and are hot spots for chromosomal rearrangements, deletions, sister chromatid exchanges and plasmid integration in response to treatment with low doses of aphidicolin (46). Rearrangements and deletions at common fragile sites are observed in cancer cells, indicating that fragile site instability may contribute to tumorigenesis (54). Indeed, both the common fragile sites FRA3B and FRA16D are located within well-characterized tumor-suppressor genes, *FHIT* and *WWOX* (46,55). In addition, replication stress induced by aphidicolin or hydroxyurea produces copy number alterations, which arise frequently in cancer cells (56). Thus, it will be of interest to further define the functions of the SNM1B nuclease activity in DNA processing at stalled replication forks and examine its roles in suppressing genomic instability, including potentially oncogenic chromosomal rearrangements.

MATERIALS AND METHODS

Knockdown of SNM1B expression by siRNA

The HCT116 colon cancer and WT fibroblast human cell lines were cultured as previously described (57). HCT116 cells were plated at a density of 1×10^5 cells per well of a six-well dish in McCoy's media (10% FBS, 1% Pen/Strep) 24 h prior to siRNA transfection. HeLa cells were plated at the same density in DMEM (10% FBS, 1% Pen/Strep). All siRNAs (50 nM) were transfected using Liptofectamine 2000 (Invitrogen) as per manufacturer's instructions. SNM1B mRNA levels were determined via semi-quantitative RT-PCR in every experiment to verify the extent of siRNA knockdown as previously described (9).

Aphidicolin sensitivity assay

WT fibroblasts transfected with NS or siSnm1B-1 (SNM1B-specific) siRNAs were plated at low density 48 h after transfection and incubated with the indicated doses of aphidicolin for 24 h. Cells were washed with media three times and allowed to recover for 5–7 days. Percent survival was determined using the colorimetric assay for cell survival as previously described (58). The sensitivity curve was performed three independent times. HeLa cells transfected with NS, siSnm1B-1 or siSnm1B-2 siRNAs and HCT116 cells transfected with NS or siSnm1B-1 siRNAs were plated and analyzed as above. The aphidicolin sensitivity curve was performed two independent times.

Chromosome anomalies and FISH

HCT116 cells transfected with NS or siSnm1B-1 were treated with aphidicolin (0.3 or 0.5 μM) for 24 h. Cells were incubated with colcemid for 1 h (untreated) or 3 h (0.3 or 0.5 μM aphidicolin). Cells were harvested and incubated in 0.075 M KCl for 15 min at 37°C followed by a series of fixations in Carnoy's fixative (3:1 methanol:acetic acid). Fixed cells were dropped onto slides and baked prior to Giemsa staining or two-color FISH. Giemsa-stained chromosomes were scored for gaps and breaks. The average gaps and breaks per metaphase were calculated from three independent experiments. For two-color FISH, probes were generated using BAC and YAC constructs containing human genomic inserts that span the fragile site regions. YAC 850A6 was used for FRA3B, and BAC26L41 was used for FRA16D (42). Probes were labeled by nick translation synthesis with digoxigenin or biotin (Roche). Two-color FISH was done as previously described (42). Approximately 30 signals were examined for each sample from at least three independent experiments. The gaps/breaks and common fragile site analyses were performed in a blinded manner. Images were acquired using a Zeiss Axioscope epifluorescence microscope and Olympus DP70 digital camera system.

Western blot analyses

HCT116 cells transfected with NS or siSnm1B-1 were treated with 0.3 μM aphidicolin for 24 h. Cells were harvested and resuspended in protein lysis buffer (25 mM HEPES, pH 7.4, 10% glycerol, 200 mM KCl, 0.1% NP40, 1 mM DTT) containing phosphatase (Roche PhosSTOP) and protease inhibitors (Roche Complete Mini EDTA-free). For the FANCD2-Ub experiments, soluble and chromatin-bound FANCD2 fractions were separated as previously described (59). Protein concentration was determined by the Bradford assay. Lysates (100 μg) were analyzed by western blotting using the appropriate primary antibodies and IRDye 800 CW secondary antibodies (Li-Cor). Bands were visualized using the Odyssey 2.1 software. All experiments were performed at least three independent times.

HCT116 cell lines expressing wild-type and mutant SNM1B were harvested and resuspended in protein lysis buffer (10 mM PIPES, pH 6.8, 100 mM NaCl, 300 mM sucrose, 1 mM $MgCl_2$, 0.1% Triton-X 100) containing phosphatase (Roche PhosSTOP) and protease inhibitors (Roche Complete Mini EDTA-free) and Benzonase (Purity >99% Novagen). Expression of SNM1B protein was analyzed by western blotting using anti-V5 antibody (Invitrogen).

Generation of HCT116 cell lines expressing siRNA-1-resistant wild-type and mutant SNM1B

An siSnm1B-1-resistant cDNA containing three silent point mutations within the siRNA-1 core sequence was used for the complementation experiments and to generate the site-specific mutants (9). The wild-type and mutant siRNA-resistant cDNAs were subcloned into the pLL-IRES-GFP lentiviral vector (UM vector core). Lentiviruses expressing the SNM1B-IRES-GFP cassettes were generated as previously described (9). HCT116 cells (2.0×10^5) were incubated with 1 ml of virus-containing media with 4 μg/ml polybrene, 1 ml of DMEM and 10% FBS for 24 h. Cells were harvested 24 h later, and the expression of the SNM1B-IRES-GFP expression cassette was determined by flow cytometry to determine the percentage of GFP-positive cells.

GFP-positive cells were sorted (University of Michigan Flow Cytometry Core), cultured and resorted. SNM1B expression levels were assessed by semi-quantitative RT-PCR using primers specific for the siRNA-resistant cDNAs. Early passage sorted cell lines with comparable levels of SNM1B expression were used for complementation experiments (Fig. 4B and 5B, Supplementary Material, Fig. S4). HCT116 cells infected with the pLL empty vector control were used for all experiments. For complementation experiments, HCT116 cells expressing wild-type or mutant SNM1B-IRES-GFP constructs were transfected with the siRNAs and FANCD2 and BRCA1 foci were quantitated in a blinded manner. Images were acquired at ×100 magnification at the same fluorescence intensity. Data represent three or more independent experiments. Error bars indicate standard error of the mean (SEM).

Immunofluorescence of subnuclear foci

HCT116 cells (4×10^4) were plated on coverslips in 12-well dishes 24 h prior to siRNA transfection. Cells were treated with aphidicolin (0.3 μM) 48 h after transfection for either 6 or 24 h. HeLa cells were plated the same way for NBS1, FANCD2 and BRCA1 foci experiments. Empty vector-IRES-GFP and WT-SNM1B-IRES-GFP HCT116 cells were plated on coverslips in 12-well dishes and then treated with aphidicolin (0.3 μM) for 24 h. For RPA, BRCA1, MRE11, NBS1 and FANCD2 foci experiments, cells were incubated in cold extraction buffer (20 mM HEPES, 50 mM NaCl, 300 mM sucrose, 3 mM $MgCl_2$, 0.5% TX-100) for 5 min followed by fixation in 3.7% *p*-formaldehyde, 2% sucrose, 0.5% TX-100 for 20 min and then washed three times with PBS. For γH2AX foci, cells were fixed in 3.7% *p*-formaldehyde, 2% sucrose for 20 min followed by incubation in cold extraction buffer for 5 min and then washed three times with PBS. For V5-SNM1B foci, cells were fixed with ice-cold 70% methanol, 30% acetone at −20°C for 20 min and then air-dried at room temperature. Cells were then stained with primary antibody for 45 min and then Alexa Fluor 488 or 594 (Invitrogen Molecular Probes) secondary antibodies for 45 min. Prolong Gold antifade reagent with DAPI (Invitrogen) was used to mount coverslips on slides. Images were acquired using the Olympus BX61 microscope and the FISHview software (Applied Spectral Imaging). At least three independent experiments were conducted.

Cell-cycle analysis

HCT116 cells were plated in a six-well dish (1×10^5 in each well) and then transfected with siRNA 24 h later. Cells were treated with 0.3 μM aphidicolin 48 h after transfection. Cells were then fixed with cold 70% ethanol, stored at −20°C overnight and stained with propidium iodide for 30 min at room temperature. FACS analysis was performed using an Accuri C6 flow cytometer and cell-cycle profiles were analyzed using the FlowJo (TreeStar) software.

Antibodies

α-pRPA32 Ser4/8 was from Bethyl (cat# A300-245A). α-pCHK1 Ser317 was from R&D Systems (cat# AF2054). α-PCNA was from Santa Cruz (PC10). α-Topoisomerase I was from BD Biosciences (cat# 556597). α-RPA and α-BRCA1 were from Calbiochem (cat# NA19L, OP92). α-γH2AX was from Millipore (cat# 05-636). α-FANCD2, α-MRE11 and α-NBS1 were from Novus Biologicals (cat# 100-182, 100-142, 110-57272). α-V5 was from Invitrogen (cat# R960-25). α-Ku70 was from Abcam (cat# 10878).

SUPPLEMENTARY MATERIAL

Supplementary Material is available at *HMG* online.

ACKNOWLEDGEMENTS

We thank Drs David Ferguson, Mats Ljungman and Tom Wilson for helpful discussions.

Conflict of Interest statement. None declared.

FUNDING

This work was supported by the National Institutes of Health (AI063058 to J.M.S.). J.M. was a predoctoral trainee on a National Institutes of Health training grant (T32-GM007544). I.D. is a predoctoral trainee on a National Institutes of Health training grant (T32-GM007315).

REFERENCES

1. Budzowska, M. and Kanaar, R. (2009) Mechanisms of dealing with DNA damage-induced replication problems. *Cell Biochem. Biophys.*, **53**, 17–31.
2. Petermann, E. and Helleday, T. (2010) Pathways of mammalian replication fork restart. *Nat. Rev. Mol. Cell Biol.*, **11**, 683–687.
3. Callebaut, I., Moshous, D., Mornon, J.P. and de Villartay, J.P. (2002) Metallo-beta-lactamase fold within nucleic acids processing enzymes: the beta-CASP family. *Nucleic Acids Res.*, **30**, 3592–3601.
4. Lam, Y., Akhter, S., Gu, P., Ye, J., Poulet, A., Giraud-Panis, M.J., Bailey, S., Gilson, E., Legerski, R. and Chang, S. (2010) SNMIB/Apollo protects leading-strand telomeres against NHEJ-mediated repair. *EMBO J.*, **29**, 2230–2241.
5. Wu, P., Takai, H. and de Lange, T. (2012) Telomeric 3′ overhangs derive from resection by Exo1 and Apollo and fill-in by POT1b-associated CST. *Cell*, **150**, 39–52.
6. Wu, P., van Overbeek, M., Rooney, S. and de Lange, T. (2010) Apollo contributes to G overhang maintenance and protects leading-end telomeres. *Mol. Cell*, **39**, 606–617.
7. Bae, J.B., Mukhopadhyay, S., Liu, L., Zhang, N., Tan, J., Akhter, S., Liu, X., Shen, X., Li, L. and Legerski, R. (2008) Snm1b/Apollo mediates replication fork collapse and S phase checkpoint activation in response to DNA interstrand cross-links. *Oncogene*, **27**, 5045–5056.

8. Demuth, I., Bradshaw, P., Lindner, A., Anders, M., Heinrich, S., Kallenbach, J., Schmelz, K., Digweed, M., Meyn, M. and Concannon, P. (2008) Endogenous hSNM1B/Apollo interacts with TRF2 and stimulates ATM in response to ionizing radiation. *DNA Repair*, **7**, 1192–1201.
9. Mason, J. and Sekiguchi, J. (2011) Snm1b/Apollo functions in the Fanconi anemia pathway in response to DNA interstrand crosslinks. *Hum. Mol. Genet.*, **20**, 2549–2559.
10. Demuth, I., Digweed, M. and Concannon, P. (2004) Human SNM1B is required for normal cellular response to both DNA interstrand crosslink-inducing agents and ionizing radiation. *Oncogene*, **23**, 8611–8618.
11. Kim, H. and D'Andrea, A.D. (2012) Regulation of DNA cross-link repair by the Fanconi anemia/BRCA pathway. *Genes Dev.*, **26**, 1393–1408.
12. Moldovan, G.L. and D'Andrea, A.D. (2009) How the Fanconi anemia pathway guards the genome. *Annu. Rev. Genet.*, **43**, 223–249.
13. Howlett, N., Taniguchi, T., Durkin, S., D'Andrea, A. and Glover, T. (2005) The Fanconi anemia pathway is required for the DNA replication stress response and for the regulation of common fragile site stability. *Hum. Mol. Genet.*, **14**, 693–701.
14. Moldovan, G.-L. and D'Andrea, A. (2012) To the rescue: the Fanconi anemia genome stability pathway salvages replication forks. *Cancer Cell*, **22**, 5–6.
15. Hashimoto, Y., Puddu, F. and Costanzo, V. (2012) RAD51- and MRE11-dependent reassembly of uncoupled CMG helicase complex at collapsed replication forks. *Nat. Struct. Mol. Biol.*, **19**, 17–24.
16. Bryant, H., Petermann, E., Schultz, N., Jemth, A.S., Loseva, O., Issaeva, N., Johansson, F., Fernandez, S., McGlynn, P. and Helleday, T. (2009) PARP is activated at stalled forks to mediate Mre11-dependent replication restart and recombination. *EMBO J.*, **28**, 2601–2615.
17. Robison, J., Elliott, J., Dixon, K. and Oakley, G. (2004) Replication protein A and the Mre11.Rad50.Nbs1 complex co-localize and interact at sites of stalled replication forks. *J. Biol. Chem.*, **279**, 34802–34810.
18. Robison, J., Lu, L., Dixon, K. and Bissler, J. (2005) DNA lesion-specific co-localization of the Mre11/Rad50/Nbs1 (MRN) complex and replication protein A (RPA) to repair foci. *J. Biol. Chem.*, **280**, 12927–12934.
19. Roques, C., Coulombe, Y., Delannoy, M., Vignard, J., Grossi, S., Brodeur, I., Rodrigue, A., Gautier, J., Stasiak, A., Stasiak, A. *et al.* (2009) MRE11-RAD50-NBS1 is a critical regulator of FANCD2 stability and function during DNA double-strand break repair. *EMBO J.*, **28**, 2400–2413.
20. Schlacher, K., Christ, N., Siaud, N., Egashira, A., Wu, H. and Jasin, M. (2011) Double-strand break repair-independent role for BRCA2 in blocking stalled replication fork degradation by MRE11. *Cell*, **145**, 529–542.
21. Ying, S., Hamdy, F. and Helleday, T. (2012) Mre11-dependent degradation of stalled DNA replication forks is prevented by BRCA2 and PARP1. *Cancer Res.*, **72**, 2814–2821.
22. Schlacher, K., Wu, H. and Jasin, M. (2012) A distinct replication fork protection pathway connects Fanconi anemia tumor suppressors to RAD51-BRCA1/2. *Cancer Cell*, **22**, 106–116.
23. Salewsky, B., Schmiester, M., Schindler, D., Digweed, M. and Demuth, I. (2012) The nuclease hSNM1B/Apollo is linked to the Fanconi anemia pathway via its interaction with FANCP/SLX4. *Hum. Mol. Genet.*, **21**, 4948–4956.
24. Andersen, S., Bergstralh, D., Kohl, K., LaRocque, J., Moore, C. and Sekelsky, J. (2009) *Drosophila* MUS312 and the vertebrate ortholog BTBD12 interact with DNA structure-specific endonucleases in DNA repair and recombination. *Mol. Cell*, **35**, 128–135.
25. Fekairi, S., Scaglione, S., Chahwan, C., Taylor, E., Tissier, A., Coulon, S., Dong, M.-Q., Ruse, C., Yates, J., Russell, P. *et al.* (2009) Human SLX4 is a Holliday junction resolvase subunit that binds multiple DNA repair/recombination endonucleases. *Cell*, **138**, 78–89.
26. Muñoz, I., Hain, K., Déclais, A.C., Gardiner, M., Toh, G., Sanchez-Pulido, L., Heuckmann, J., Toth, R., Macartney, T., Eppink, B. *et al.* (2009) Coordination of structure-specific nucleases by human SLX4/BTBD12 is required for DNA repair. *Mol. Cell*, **35**, 116–127.
27. Svendsen, J., Smogorzewska, A., Sowa, M., O'Connell, B., Gygi, S., Elledge, S. and Harper, J. (2009) Mammalian BTBD12/SLX4 assembles a Holliday junction resolvase and is required for DNA repair. *Cell*, **138**, 63–77.
28. Shimura, T., Torres, M., Martin, M., Rao, V., Pommier, Y., Katsura, M., Miyagawa, K. and Aladjem, M. (2008) Bloom's syndrome helicase and Mus81 are required to induce transient double-strand DNA breaks in response to DNA replication stress. *J. Mol. Biol.*, **375**, 1152–1164.
29. Zou, L. and Elledge, S. (2003) Sensing DNA damage through ATRIP recognition of RPA-ssDNA complexes. *Science*, **300**, 1542–1548.
30. Liu, Q., Guntuku, S., Cui, X., Matsuoka, S., Cortez, D., Tamai, K., Luo, G., Carattini-Rivera, S., DeMayo, F., Bradley, A. *et al.* (2000) Chk1 is an essential kinase that is regulated by Atr and required for the G(2)/M DNA damage checkpoint. *Genes Dev.*, **14**, 1448–1459.
31. Haracska, L., Unk, I., Johnson, R., Phillips, B., Hurwitz, J., Prakash, L. and Prakash, S. (2002) Stimulation of DNA synthesis activity of human DNA polymerase kappa by PCNA. *Mol. Cell. Biol.*, **22**, 784–791.
32. Yang, X., Shiotani, B., Classon, M. and Zou, L. (2008) Chk1 and Claspin potentiate PCNA ubiquitination. *Genes Dev.*, **22**, 1147–1152.
33. Sirbu, B., Couch, F., Feigerle, J., Bhaskara, S., Hiebert, S. and Cortez, D. (2011) Analysis of protein dynamics at active, stalled, and collapsed replication forks. *Genes Dev.*, **25**, 1320–1327.
34. Ward, I. and Chen, J. (2001) Histone H2AX is phosphorylated in an ATR-dependent manner in response to replicational stress. *J. Biol. Chem.*, **276**, 47759–47762.
35. Bogliolo, M., Lyakhovich, A., Callén, E., Castellá, M., Cappelli, E., Ramírez, M.J., Creus, A., Marcos, R., Kalb, R., Neveling, K. *et al.* (2007) Histone H2AX and Fanconi anemia FANCD2 function in the same pathway to maintain chromosome stability. *EMBO J.*, **26**, 1340–1351.
36. Oakley, G., Tillison, K., Opiyo, S., Glanzer, J., Horn, J. and Patrick, S. (2009) Physical interaction between replication protein A (RPA) and MRN: involvement of RPA2 phosphorylation and the N-terminus of RPA1. *Biochemistry*, **48**, 7473–7481.
37. Joo, W., Xu, G., Persky, N., Smogorzewska, A., Rudge, D., Buzovetsky, O., Elledge, S. and Pavletich, N. (2011) Structure of the FANCI-FANCD2 complex: insights into the Fanconi anemia DNA repair pathway. *Science*, **333**, 312–316.
38. Smogorzewska, A., Matsuoka, S., Vinciguerra, P., McDonald, E., Hurov, K., Luo, J., Ballif, B., Gygi, S., Hofmann, K., D'Andrea, A. *et al.* (2007) Identification of the FANCI protein, a monoubiquitinated FANCD2 paralog required for DNA repair. *Cell*, **129**, 289–301.
39. Lenain, C., Bauwens, S., Amiard, S., Brunori, M., Giraud-Panis, M.J. and Gilson, E. (2006) The Apollo 5′ exonuclease functions together with TRF2 to protect telomeres from DNA repair. *Curr. Biol.*, **16**, 1303–1310.
40. Sengerova, B., Allerston, C.K., Abu, M., Lee, S.Y., Hartley, J., Kiakos, K., Schofield, C.J., Hartley, J.A., Gileadi, O. and McHugh, P.J. (2012) Characterization of the human SNM1A and SNM1B/Apollo DNA repair exonucleases. *J. Biol. Chem.*, **287**, 26254–26267.
41. Ye, J., Lenain, C., Bauwens, S., Rizzo, A., Saint-Léger, A., Poulet, A., Benarroch, D., Magdinier, F., Morere, J., Amiard, S. *et al.* (2010) TRF2 and Apollo cooperate with topoisomerase 2alpha to protect human telomeres from replicative damage. *Cell*, **142**, 230–242.
42. Arlt, M., Xu, B., Durkin, S., Casper, A., Kastan, M. and Glover, T. (2004) BRCA1 is required for common-fragile-site stability via its G2/M checkpoint function. *Mol. Cell. Biol.*, **24**, 6701–6709.
43. Casper, A., Nghiem, P., Arlt, M. and Glover, T. (2002) ATR regulates fragile site stability. *Cell*, **111**, 779–789.
44. Durkin, S., Arlt, M., Howlett, N. and Glover, T. (2006) Depletion of CHK1, but not CHK2, induces chromosomal instability and breaks at common fragile sites. *Oncogene*, **25**, 4381–4388.
45. Akhter, S., Lam, Y., Chang, S. and Legerski, R. (2010) The telomeric protein SNM1B/Apollo is required for normal cell proliferation and embryonic development. *Aging Cell*, **9**, 1047–1056.
46. Durkin, S. and Glover, T. (2007) Chromosome fragile sites. *Annu. Rev. Genet.*, **41**, 169–192.
47. Errico, A. and Costanzo, V. (2012) Mechanisms of replication fork protection: a safeguard for genome stability. *Crit. Rev. Biochem. Mol. Biol.*, **47**, 222–235.
48. Franchitto, A. and Pichierri, P. (2011) Understanding the molecular basis of common fragile sites instability: role of the proteins involved in the recovery of stalled replication forks. *Cell Cycle*, **10**, 4039–4046.
49. Jones, R. and Petermann, E. (2012) Replication fork dynamics and the DNA damage response. *Biochem. J.*, **443**, 13–26.
50. Costanzo, V. (2011) Brca2, Rad51 and Mre11: performing balancing acts on replication forks. *DNA Repair*, **10**, 1060–1065.
51. Postow, L., Crisona, N., Peter, B., Hardy, C. and Cozzarelli, N. (2001) Topological challenges to DNA replication: conformations at the fork. *Proc. Natl Acad. Sci. USA*, **98**, 8219–8226.
52. Hanada, K., Budzowska, M., Davies, S., van Drunen, E., Onizawa, H., Beverloo, H., Maas, A., Essers, J., Hickson, I. and Kanaar, R. (2007) The structure-specific endonuclease Mus81 contributes to replication restart by

generating double-strand DNA breaks. *Nat. Struct. Mol. Biol.*, **14**, 1096–1104.
53. Regairaz, M., Zhang, Y.W., Fu, H., Agama, K., Tata, N., Agrawal, S., Aladjem, M. and Pommier, Y. (2011) Mus81-mediated DNA cleavage resolves replication forks stalled by topoisomerase I-DNA complexes. *J. Cell Biol.*, **195**, 739–749.
54. Ozeri-Galai, E., Bester, A.C. and Kerem, B. (2012) The complex basis underlying common fragile site instability in cancer. *Trends Genet.*, **28**, 295–302.
55. Pichiorri, F., Ishii, H., Okumura, H., Trapasso, F., Wang, Y. and Huebner, K. (2008) Molecular parameters of genome instability: roles of fragile genes at common fragile sites. *J. Cell Biochem.*, **104**, 1525–1533.
56. Arlt, M.F., Ozdemir, A.C., Birkeland, S.R., Wilson, T.E. and Glover, T.W. (2011) Hydroxyurea induces de novo copy number variants in human cells. *Proc. Natl Acad. Sci. USA*, **108**, 17360–17365.
57. Timmers, C., Taniguchi, T., Hejna, J., Reifsteck, C., Lucas, L., Bruun, D., Thayer, M., Cox, B., Olson, S., D'Andrea, A. *et al.* (2001) Positional cloning of a novel Fanconi anemia gene, FANCD2. *Mol. Cell*, **7**, 241–248.
58. Taniguchi, T., Garcia-Higuera, I., Xu, B., Andreassen, P., Gregory, R., Kim, S.T., Lane, W., Kastan, M. and D'Andrea, A. (2002) Convergence of the Fanconi anemia and ataxia telangiectasia signaling pathways. *Cell*, **109**, 459–472.
59. Kim, J., Kee, Y., Gurtan, A. and D'Andrea, A. (2008) Cell cycle-dependent chromatin loading of the Fanconi anemia core complex by FANCM/FAAP24. *Blood*, **111**, 5215–5222.